A MILP-based Restoration Planning Method for Generator Start-up Considering Flexible Re-energizing Times of Transmission Lines

Xie, Yunyun; Li , Dezheng; Xu, Yan; Wu, Qiuwei; Yin, Minghui

Published in:
International Journal of Electrical Power & Energy Systems

Link to article, DOI:
10.1016/j.ijepes.2020.106357

Publication date:
2020

Document Version
Peer reviewed version

Available online at www.sciencedirect.com

SciVerse ScienceDirect

00 (2012) 000–000

A MILP-based Restoration Planning Method for Generator Start-up Considering Flexible Re-energizing Times of Transmission Lines

Yunyun Xie [a], Dezheng Li [b], Yan Xu [c], Qiuwei Wu [d], Minghui Yin [a]

[a] *School of Automation, Nanjing University of Science and Technology, Nanjing 210094, Jiangsu Province, China*
[b] *State Grid Liaocheng Power Supply Company, Liaocheng 252000, Shandong Province, China*
[c] *Nanyang Technological University, Singapore*
[d] *Centre for Electric Power and Energy, Technical University of Denmark, Kgs. Lyngby, DK 2800*

Abstract

During power system restoration, the planning of the generator start-up sequence (GSUS) can significantly affect the restoration efficiency. However, a GSUS optimization model based on mixed integer linear programming (MILP) cannot satisfy the need for flexible re-energizing times of transmission liens and the serial restoration of generators. To solve this issue, a new MILP-based GSUS optimization model is proposed in this paper that can generate a serial GSUS scheme with flexible re-energizing times of transmission lines. The requirements of flexible re-energizing times of transmission lines and the serial restoration of the generators are formulated as restoration time constraints for the transmission lines, start-up time constraints for the buses on the restoration paths, and a serial restoration constraint, which are transformed into mixed integer linear constraints by means of auxiliary binary (0-1) decision variables. Meanwhile, the restart time constraints of the generators and the transient frequency requirements are modeled as mixed integer linear constraints. Finally, the performance of the proposed method is verified on the IEEE 39-bus system.

Key Words: power system restoration, mixed integer linear programming, generator start-up sequence.

Nomenclature

A. Indices and Sets

Ω^G Set of generators.
Ω_t^L Set of restored transmission lines at time t.
Ω_t^B Set of restored buses at time t.
Ω^{BUS} Set of buses.
Ω^{bus} Set of buses that are not connected to generators.
Ω_r^G Set of restored generators.
Ω_k^G Set of generators whose restoration paths include bus k.
Ω_m^{res} Set of buses that can be used to restart generator m.
T End time for system restoration.
T^L Set of time intervals for line restoration operations.
T^G Set of time intervals for generator start-up.

ε Sufficiently small positive numbers to make the corresponding constraints take certain values.

B. Parameters

$P_{g,t}^{crank}$ Cranking power for restarting generator g at time *t.*

V^{TL} Length of each time interval in T^L.

V^{T} Length of each time interval in T^G.

C_g Power required to restart generator *g*.

P_g Rated power of generator *g*.

T_g^R Ramping time of generator *g*.

T_g^C Cranking time of generator *g*.

$T_g^{\min}$ Minimum cold restart time of generator *g*.

$T_g^{\max}$ Maximum hot restart time of generator *g*.

R_g Ramping rate of generator *g*.

T Time of system restoration.

f_N Rated frequency.

$\Delta f_{\lim}$ Upper-limit frequency deviation.

df_g Dynamic frequency response coefficient of restored generator *g*.

C. Variables

E^{sys} Total energy generated during system restoration.

E_g^{crank} Energy required for the start-up of generator *g*.

E_g^{gen} Energy generated by generator *g*.

$P_{g,t}^{gen}$ Power of generator *g* at time *t.*

t_g^{start} Start-up time of generator *g*.

t_m^{start} Start-up time of generator *m*.

t_i^{start} Start-up time of bus *i*.

t_k^{start} Start-up time of bus *k*.

$u_{Lij,t}$ Binary variable related to the restoration status of line *i*-*j* at time *t*.

$u_{Lij,t-1}$ Binary variable related to the restoration status of line *i*-*j* at time *t*-1.

$u_{i,t}$ Binary variable related to the restoration status of bus *i* at time *t*.

$u_{i,t-1}$ Binary variable related to the restoration status of bus *i* at time *t*-1.

$u_{j,t-1}$ Binary variable related to the restoration status of bus *j* at time *t*-1.

t_m^{path} Start-up time for the restoration path to restart generator *m*.

b_{im} Binary variable for choosing the restoration path.

$a_{im}^{(1)}$, $a_{im}^{(2)}$ Binary variables related to the restoration state of bus *i* when generator *m* starts.

$a_{km}^{(2)}$ Binary variable related to the restoration state of bus *k* when generator *m* starts.

d_{mk}, e_k Binary variable that determines the start-up time for bus *k* on the restoration path.

$e_g^{(1)}$, $e_g^{(2)}$ Binary variables for implementing one of the two constraints.

$e_{gm}^{(1)}$, $e_{gm}^{(2)}$ Binary variables for implementing one of the two constraints at the start-up time of generator *m*.

$z_g^{(i)}$ Four auxiliary binary variables related to the restoration status of generator *g*.

T_{im} Shortest restoration time from bus *i* to generator *m*, which can be generated by the *Floyd* algorithm.

T_{kj} Shortest restoration time between bus *k* and generator *m*.

T_{ij} Shortest restoration time between generator *i* and generator *m*.

$B(i,m)$ Matrix related to the shortest restoration time between bus *i* and generator *m*.

$D(i,m)$ Matrix related to the candidate restoration paths for non-black-start (NBS) generator *m*.

M_x Sufficiently large positive numbers to make the corresponding constraints completely redundant when the binary variables take certain values.

$z_{gm}^{(i)}$ Four auxiliary binary variables related to the restoration status of generator g at the start-up time of generator m.

$z_{mm}^{(2)}$ Binary variables related to whether generator m is in the cranking period.

1. Introduction

Although the operational efficiency and reliability of a power system are improved by extensive interconnectivity of the power network, the static and dynamic behaviors of an large-scale interconnected power system also become more complex and unpredictable due to growing integration of low-inertia sources, operation in the vicinity of the maximum limits, and capacities below market outlooks, et al, which increase the risk of blackouts. Large-area blackouts resulting from occasional failures caused by contingencies or extreme weather events can result in enormous economic and social costs [1]. In July 2012, the world's worst blackout in history occurred in India, leaving more than 700 million people in 28 states without power [2]. A major blackout in South Australia in 2016 was caused by a shutdown of wind power [3]. In addition to those mentioned above, many other blackouts have also occurred around the world in recent years, such as the Brazilian blackout in 2018 [4] and the Argentinian blackout in 2019 [5]. After such a large-area blackout, an effective restoration scheme can significantly reduce the load outage time, ensure security during restoration, and improve the resilience of the power system [6]. Therefore, restoration planning is important for successful power restoration.

Power system restoration is a complex process involving multiple objectives and constraints on multiple timescales. Generally, the restoration procedure is divided into three stages: preparation, system restoration and load restoration [7]. The main objective in the preparation stage is to sectionalize the blacked-out system into subsystems according to its topology and the locations of the black-start (BS) generators. The availability of power sources and transmission lines was assessed based on the information provided by the wide-area measurement system (WAMS) in [8][9]. The blackout system can be sectionalized using multiple methods, such as graph theory [10], ordered binary decision diagram (OBDD) method [11], or complex network theory [12], et al. After the preparation stage, system restoration is carried out in each subsystem simultaneously to restart the non-black-start (NBS) generators and sequentially restore the transmission lines [13]. A two-stage optimization model was proposed in [14] for optimizing the network configuration, firstly for the NBS generator start-up sequence (GSUS) and then for the restoration paths. A decentralized restoration scheme was presented in [15] to realize the coordinated restoration of transmission and distribution systems. Various new energy sources, such as electric vehicles and energy storage systems, were employed as power sources during system restoration in [16][17]. In the final load restoration stage, the objective is to maximize the load pickup for given bus voltage and frequency thresholds. In [18], a hierarchical response-based method was proposed to maximize the amount of load pickup. Wind energy was employed to increase the amount of load pickup in [19][20].

Restoration planning for the GSUS in the system restoration stage can directly affect restoration efficiency and system security; consequently, it has attracted considerable attention from researchers. Since system restoration planning for the GSUS is a complicated optimal decision-making problem with multiple objectives (minimizing the restoration time and maximizing the generation capacity) and various operational and technical constraints (self-excitation constraints for the generators, sustained and transient overvoltage constraints for the transmission lines, a transient frequency constraint, etc.), early studies focused on the use of expert systems to generate restoration schemes [21][22][23]. However, although expert systems can produce useful heuristic restoration rules, they are suitable only for specific systems and provide limited quantitative analysis capabilities. To generate better restoration schemes, the problem of system restoration

planning has been modeled as a nonlinear multi-constraint mathematical planning problem in many studies [24][25][26]. For example, the system restoration problem has been formulated as a permutation-based combinatorial optimization problem [24]. Nonlinear mathematical planning models are usually solved using meta-heuristic algorithms, such as differential evolutionary algorithms [24], the firefly algorithm [25], or genetic algorithms [26]. However, these heuristic methods often converge to locally optimal solutions, and they have a low solution efficiency and cannot guarantee solution convergence.

The main challenge in efficiently solving a restoration planning model for a GSUS is the coupling between the GSUS and the transmission line re-energizing sequence. The start-up time for an NBS generator is constrained by the re-energizing time for the restoration path that connects that NBS generator to the power source. A restoration path must pass through each of the NBS generators. Consequently, in some studies, the restoration planning problem has been decoupled into two separate optimization problems to improve the solution efficiency. Reference [27] proposed a two-stage method of restoration scheme generation, in which the optimization of the GSUS in the first stage is coordinated with the optimization of the re-energizing of the transmission lines in the second stage. However, the optimization model for the GSUS is still nonlinear and thus is not easy to solve. In [28], the GSUS planning problem was formulated as a mixed integer linear programming (MILP) problem. In [29], a MILP-based integrated restoration model was proposed for sectionalization and GSUS optimization. Although the above MILP models can be solved effectively, optimizing the two problems separately decreases the efficiency of system restoration. Therefore, some researchers have established integrated models for generator start-up and transmission line re-energizing. The GSUS planning problem was formulated as a linear integer programming problem using a new generator model in [30] and was formulated as a MILP model considering the transmission line re-energizing sequence in [31]. In these studies, the re-energizing time for each transmission line was considered to be a constant time interval. However, since the re-energizing time may vary for different transmission lines, for practical system restoration problems, it is more reasonable to consider flexible re-energizing times. Although flexible re-energizing times have not been considered in existing studies, this requirement has been presented in many papers [14,24,30]. Additionally, the restoration of the NBS generators has been assumed to occur in parallel, although the restoration of the generators and transmission lines in the system restoration stage is usually performed in a sequential manner. Consequently, the current methods cannot satisfy the need to consider flexible times for transmission line restoration and generate a serial restoration scheme.

In most of the existing works [21]-[26], the GSUS planning problem has been formulated as a nonlinear multi-constraint planning problem, and metaheuristic algorithms have been employed to solve the corresponding nonlinear models; however, such algorithms have a low solution efficiency and cannot guarantee solution convergence. In [28]-[31], the GSUS planning problem was transformed into a MILP problem to improve the solution efficiency. However, the corresponding models also cannot satisfy the need to consider flexible times for transmission line restoration and generate a serial restoration scheme.

Based on the above discussions, this paper proposes a novel MILP-based restoration planning model for a serial GSUS considering flexible re-energizing times for transmission lines. The contributions of the proposed model are summarized as follows:

1) The GSUS is optimized considering the need for flexible re-energizing times for the transmission lines and the serial restoration of the generators.

2) The flexible re-energizing time and serial restoration requirements are formulated as restoration time constraints for the transmission lines, start-up time constraints for the buses on the restoration paths, and a serial restoration constraint.

3) The restoration time constraints for the transmission lines, the start-up time constraints for the buses on the restoration paths, and the serial restoration constraint are transformed into mixed integer linear constraints by means of auxiliary binary (0-1) decision variables.

4) The transient frequency requirement is modeled as a series of mixed integer linear constraints.

5) The maximum and minimum restart time constraints are simultaneously expressed in a single model.

The remainder of this paper is organized as follows. The framework for system restoration planning is introduced in Section 2. Section 3 presents the GSUS optimization model, which considers flexible re-energizing times for the transmission lines. The solution method for the proposed model is proposed in Section 4. Case study results are presented in Section 5, followed by the conclusions.

2. Framework and Problem Description of System Restoration Planning

System restoration planning is a complicated optimal decision-making problem with nonlinear operational and technical constraints; hence, it is difficult to solve efficiently. In the current research [29][31], this optimization problem is decomposed into three subproblems: GSUS optimization, transmission line re-energizing sequence optimization, and generator dispatch and load pickup. These three subproblems are solved iteratively to generate a restoration plan that is technically feasible. The framework for system restoration planning is illustrated in Fig. 1.

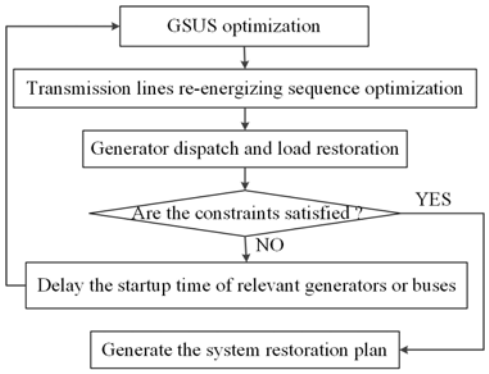

Fig. 1 Framework for system restoration planning

In the first subproblem, the GSUS is optimized, while the network topology constraints and the operational and technical constraints are ignored [28]. The second subproblem generates the re-energizing sequence for the transmission lines based on the GSUS. Then, in the third subproblem, generator dispatch and load restoration are carried out considering the operational and technical constraints. When a constraint is violated, a few options can be applied to repair the restoration plan, such as using reactive power compensation devices or delaying the start-up times of certain generators and buses to generate a new start-up sequence [28,29].

Because the separate optimization of the first two subproblems decreases the efficiency of system restoration, integrated models for these two subproblems were reported in [30][31], which can be formulated as follows:

$$\max E^{sys} = \sum_{g \in \Omega^G} (E_g^{gen} - E_g^{crank}) \tag{1}$$

subject to

$$\sum_{g \in \Omega^G} (P_{g,t}^{gen} - P_{g,t}^{crank}) \geq 0, \ \forall t \in T^G \tag{2}$$

$$t_g^{start} \le T_g^{\max} \tag{3}$$

$$t_g^{start} \ge T_g^{\min} \tag{4}$$

$$V^{TL}(\sum_{t\in T^L}(1-u_{i,t})+1) = V^T t_g^{start}, \forall i \in \Omega^{BUS} \tag{5}$$

$$u_{Lij,t} \le u_{i,t-1} + u_{j,t-1}, \forall L_{ij} \in \Omega_t^L, t \in T^L \tag{6}$$

$$u_{i,t} \le u_{Lij,t}, \forall i \in \Omega_t^B, t \in T^L \tag{7}$$

$$u_{i,t-1} \le u_{i,t}, u_{Lij,t-1} \le u_{Lij,t}, \forall i \in \Omega_t^B, L_{ij} \in \Omega_t^L, t \in T^L \tag{8}$$

In the above formulation, the objective function (1) maximizes the energy generated during system restoration. The first term in (1) represents the energy generated by generator *g* during system restoration. The second term in (1) represents the energy required for the start-up of generator *g*. This objective function ensures that the restored generators generate as much energy as possible to restore the loads that are in outage. Constraint (2) guarantees that the power produced by the restored generators satisfies the start-up power requirement of the NBS generators. Constraints (3) and (4) represent the start-up time requirements of the NBS generators. A thermal generator can be restarted within a maximum restart time of $T_g^{\max}$ after the generator has shut down. After this maximum restart time, the generator cannot be restarted until the minimum cold start-up time $T_g^{\min}$ has passed. Constraint (5) guarantees that generator *g* is restarted following its connected bus *i*. Constraints (6) and (7) guarantee that transmission line L_{ij} is re-energized after its connected bus is restored. Constraint (8) states that a transmission line or bus will not be energized again once it is energized. Constraints (5)-(8) can only be applied in parallel for transmission lines with the same restoration time.

Because the typical generator capacity curve is a nonlinear curve consisting of four piecewise linear functions, Eqns. (1) and (4) are nonlinear and were transformed into a MILP model in [29][30][31]. In addition, the topology and state constraints of the buses and lines were simultaneously expanded for the new model. However, the restoration time for the transmission lines and buses is determined by the time interval for transmission line re-energizing. When the re-energizing times for different transmission lines are different, this method will not work. Additionally, the topology and state constraints do not permit the generation of a serial restoration scheme.

3. Proposed Mathematical Modeling

In this section, the objective function and the constraints for the GSUS optimization model are transformed into a MILP model that considers flexible re-energizing times for the transmission lines and the serial restoration of the generators.

3.1. Modeling principle

Since GSUS optimization is a combinatorial optimization problem and restoration path optimization is a shortest-path optimization problem, it is challenging to directly integrate the re-energizing times of the transmission lines into the GSUS optimization model. However, during system restoration, the re-energizing of the transmission lines is equivalent to the re-energizing of the connected buses. Therefore, the re-

energizing times of the transmission lines can be considered equivalent to re-energizing time constraints for the connected buses. Moreover, the connection relationships and the shortest paths between different buses can be treated as initial conditions for GSUS optimization, thereby simplifying the restoration path optimization problem. Consequently, the re-energizing times of the transmission lines can be considered in the GSUS optimization model in the form of re-energizing time constraints on the connected buses, as proposed in this paper.

3.2. Generator capacity curve model

The generator capacity curve is the basis of GSUS optimization. The capacity curve for an NBS generator [29] is shown in Fig. 2, where the start-up time of the generator is t_g^{start}, which is the decision variable. Following t_g^{start} is the cranking time T_g^C, during which the generator only consumes a constant cranking power C_g without producing any power. The time period T_g^R following the cranking period T_g^C is a ramping period during which the generator produces power and ramps up at rate R_g until it reaches its maximum power output P_g, which is determined by the installed capacity of the generator. For a BS generator, the start-up time t_g^{start} is 0.

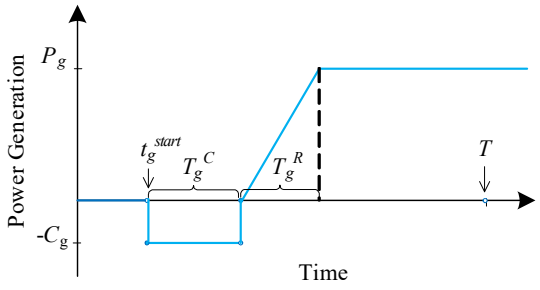

Fig. 2 Generator capacity curve

In the current research, the generator capacity curve is usually modeled as a piecewise linear function [18-20], which can be expressed as follows:

$$P(t)=\begin{cases}0 & 0\le t<t_g^{start}\\ -C_g & t_g^{start}\le t<t_g^{start}+T_g^C\\ R_g\left(t-t_g^{start}-T_g^C\right) & t_g^{start}+T_g^C\le t<t_g^{start}+T_g^C+T_g^R\\ P_g & t_g^{start}+T_g^C+T_g^R\le t<T\end{cases} \tag{9}$$

This piecewise linear function is a nonlinear model and thus needs to be transformed into a linear model. Four auxiliary binary variables are introduced to linearize the model [29], as follows:

$$P(t)=0+(-C_g)z_g^{(2)}+R_g(t-t_g^{start}-T_g^C)z_g^{(3)}+P_g z_g^{(4)} \tag{10}$$

$$z_g^{(1)}+z_g^{(2)}+z_g^{(3)}+z_g^{(4)}=1 \tag{11}$$

$$0\le t\le t_g^{start}+(1-z_g^{(1)})M_1 \tag{12}$$

$$t_g^{start} - (1 - z_g^{(2)})M_2 \le t \le t_g^{start} + T_g^C + (1 - z_g^{(2)})M_3 \tag{13}$$

$$t_g^{start} + T_g^C - (1 - z_g^{(3)})M_4 \le t \le t_g^{start} + T_g^C + T_g^R + (1 - z_g^{(3)})M_5 \tag{14}$$

$$t_g^{start} + T_g^C + T_g^R - (1 - z_g^{(4)})M_6 \le t \le T \tag{15}$$

where $z_g^{(1)}$, $z_g^{(2)}$, $z_g^{(3)}$, and $z_g^{(4)}$ are four auxiliary binary (0-1) variables, each associated with one of the four segments of the generator capacity function. These four auxiliary variables determine the restoration period for the NBS generator. In this paper, the big-M method is used to set the values M_x (x=1,2,⋯) as positive numbers that are sufficiently large to make the corresponding constraints redundant when the binary variables take certain values. In the big-*M* method, the value of M_x must be larger than the values of other variables. However, if it is too large, the computational efficiency will be reduced. A suitable value of M_x can be determined using the method presented in [29]. Here, taking M_1 and M_2 as examples, since all generators can be restarted in 130 min in the case considered in this paper, the values of M_1 and M_2 can be set to 150.

At most one auxiliary variable may be positive at time *t* to ensure that the time *t* is located in only one segment of the curve; for example, when *t* is located in the cranking period, $t \in [t_g^{start}, t_g^{start} + T_g^C)$, $z_g^{(2)} = 1$, and the other auxiliary variables are equal to zero.

3.3. Objective function

The objective function is a nonlinear function due to the nonlinearity of the generator capacity curve. The objective function can be transformed into Eqn. (16). For a description of the transformation method, the reader is referred to [28].

$$\max E^{\text{sys}} \Leftrightarrow \min \sum_{g \in \Omega^G} P_g t_g^{start} \tag{16}$$

The transformed objective function is a linear function related to the generator start-up times, t_g^{start}.

3.4. Start-up power requirement constraint

Based on the linearized model of the generator capacity curve, the start-up power requirement constraint (2) can be transformed into Eqns. (17)-(22) as follows [29]:

$$\sum_{g \in \Omega^G} (-C_g z_{gm}^{(2)} + R_g (t_m^{start} - t_g^{start} - T_g^C) z_{gm}^{(3)} + P_g z_{gm}^{(4)}) \ge 0 \quad \forall m \in \Omega^G \tag{17}$$

$$z_{gm}^{(1)} + z_{gm}^{(2)} + z_{gm}^{(3)} + z_{gm}^{(4)} = 1 \quad \forall g \in \Omega^G, m \in \Omega^G \tag{18}$$

$$0 \le t_m^{start} + \varepsilon \le t_g^{start} + (1 - z_{gm}^{(1)})M_1 \quad \forall g \in \Omega^G, m \in \Omega^G \tag{19}$$

$$t_g^{start} - (1 - z_{gm}^{(2)})M_2 \le t_m^{start} + \varepsilon \le t_g^{start} + T_g^C + (1 - z_{gm}^{(2)})M_3 \quad \forall g \in \Omega^G, m \in \Omega^G \tag{20}$$

$$t_g^{start} + T_g^C - (1 - z_{gm}^{(3)})M_4 \le t_m^{start} + \varepsilon \le t_g^{start} + T_g^C + T_g^R + (1 - z_{gm}^{(3)})M_5 \quad \forall g \in \Omega^G, m \in \Omega^G \tag{21}$$

$$t_g^{start} + T_g^C + T_g^R - (1 - z_{gm}^{(4)})M_6 \le t_m^{start} + \varepsilon \le T \quad \forall g \in \Omega^G, m \in \Omega^G \tag{22}$$

where $z_{gm}^{(x)}$ (x=1,2,3,4) is an auxiliary binary (0-1) variable that specifies the restoration status of generator g at the start-up of generator m and ε is a small positive number that helps avoid the evaluation of the start-up power requirement constraint at time t_m^{start} because the generator capacity curve is not continuous at time t_m^{start}. Eqns. (17)-(22) are checked at every time point t_m^{start}.

In constraint (17), $t_m^{start} z_{gm}^{(3)}$ and $t_g^{start} z_{gm}^{(3)}$ are nonlinear terms, which can be linearized by introducing two auxiliary variables ω_{gm} and v_{gm} [29]. Let $w_{gm}=t_g^{start} z_{gm}^{(3)}$ and $v_{gm}=t_m^{start} z_{gm}^{(3)}$. The linearization is as follows.

$$w_{gm} \le z_{gm}^{(3)} M_7 \tag{23}$$

$$t_g^{start} + (z_{gm}^{(3)} - 1)M_8 \le w_{gm} \le t_g^{start} + (1 - z_{gm}^{(3)})M_9 \tag{24}$$

$$v_{gm} \le z_{gm}^{(3)} M_{10} \tag{25}$$

$$t_m^{start} + (z_{gm}^{(3)} - 1)M_{11} \le v_{gm} \le t_m^{start} + (1 - z_{gm}^{(3)})M_{12} \tag{26}$$

With the introduction of w_{gm} and v_{gm}, constraint (17) becomes

$$\sum_{g \in \Omega^G} (-C_g z_{gm}^{(2)} + R_g (v_{gm} + \varepsilon - w_{gm} - T_g^C z_{gm}^{(3)}) + P_g z_{gm}^{(4)}) \ge 0 \ \forall m \in \Omega^G \tag{27}$$

3.5. Restoration time constraints for transmission lines

The start-up time for NBS generator m must be later than the start-up time for the restoration path of generator m plus the re-energizing time of the restoration path. Consequently, the start-up time for generator m can be expressed as follows.

$$t_m^{start} \ge t_m^{path} + T_{im} b_{im} \ \forall i \in \Omega^G \cup \Omega^{bus}, m \in \Omega^G \tag{28}$$

Eqn. (28) is used to formulate the start-up times of the generators considering the re-energizing times of the transmission lines. When b_{im} = 1, the path between bus i and generator m is chosen as the restoration path, and the restoration time of the shortest restoration path is added to the start-up time of generator m. Because generator m can be restored by only one path, b_{im} should be constrained as follows:

$$\sum_{i \in \Omega_m^{res}} b_{im} = 1, \ \forall m \in \Omega^G \tag{29}$$

The start-up time for the restoration path to restart generator m must be later than the start-up time of the initial bus i on the restoration path; this can be expressed as follows:

$$t_m^{path} \ge t_i^{start} - a_{im}^{(1)} M_{11}, \ \forall i \in \Omega^G \cup \Omega^{bus}, m \in \Omega^G \tag{30}$$

When $a_{im}^{(1)}$=0, bus i has been re-energized, and the constraint is valid. When $a_{im}^{(1)} = 1$, the constraint is invalid. Moreover, only a restored bus can be used as the initial bus of the restoration path; this can be expressed as follows:

$$b_{im} \le a_{im}^{(2)}, \ \forall i \in \Omega^G \cup \Omega^{bus}, m \in \Omega^G \tag{31}$$

The relationship between $a_{im}^{(1)}$ and $a_{im}^{(2)}$ is

$$a_{im}^{(1)}+a_{im}^{(2)}=1,\ \forall i \in \Omega^G \cup \Omega^{bus}, m \in \Omega^G \tag{32}$$

Based on bus states $a_{im}^{(1)}$ and $a_{im}^{(2)}$, the relationship between the start-up times of generator *m* and the initial bus *i* can be expressed as

$$0 \le t_m^{start} + \varepsilon \le t_i^{start} + (1-a_{im}^{(1)})M_{12} \ \ \forall m \in \Omega^G, i \in \Omega^G \cup \Omega^{bus} \tag{33}$$

$$t_i^{start} - (1-a_{km}^{(2)})M_{13} \le t_m^{start} + \varepsilon \le T \ \forall m \in \Omega^G, i \in \Omega^G \cup \Omega^{bus} \tag{34}$$

When the initial bus *i* is not energized ($a_{im}^{(1)}=1$), its re-energizing time will be later than the start-up time of generator *m*. When bus *i* is energized ($a_{im}^{(1)}=0$), its re-energizing time will be earlier than the start-up time of generator *m*.

3.6. Start-up time constraints for buses on a restoration path

In addition to the start-up times of the initial and end buses on the restoration path, the start-up times of the other buses on the restoration path should also be constrained. The start-up times for buses on the restoration path must be earlier than the start-up time of NBS generator *m*, which can be expressed as follows.

$$t_m^{start} - t_k^{start} \le d_{mk}M_{14},\ \forall m \in \Omega_k^G, k \in \Omega^{bus} \tag{35}$$

$$t_k^{start} - t_m^{start} \le d_{mk}M_{14},\ \forall m \in \Omega_k^G, k \in \Omega^{bus} \tag{36}$$

$$M_{15} - t_k^{start} \le e_k M_{16},\ \forall k \in \Omega^{bus} \tag{37}$$

$$t_k^{start} - M_{15} \le e_k M_{16},\ \forall k \in \Omega^{bus} \tag{38}$$

$$\sum_{m=1}^{f_k} d_{mk} + e_k = f_k,\ \ \forall m \in \Omega_k^G, k \in \Omega^{bus} \tag{39}$$

When $d_{mk}=0$, the start-up time for bus *k* is equal to the start-up time for generator *m*, which means that bus *k* is on the restoration path; otherwise, it is equal to M_{15}, which means that bus *k* has not been restarted. M_{15} should be smaller than M_{16}. Eqn. (39) ensures that bus *k* is located on only one restoration path if it is re-energized.

There may be several restoration paths including bus *k* that satisfy Eqns. (35)-(39). Consequently, the start-up time for bus *k* should be further constrained to be within the restoration path of the generator, which can be expressed as follows.

$$t_k^{start} \ge t_m^{start} + 1 - \sum_{m \in \Omega_k^G} b_{im} - M_{17}a_{km}^{(2)} \ \ \forall i \in \Omega^G \cup \Omega^{bus}, k \in \Omega^{bus} \tag{40}$$

$$t_k^{start} \le t_m^{start} + M_{18}(1 - \sum_{m \in \Omega_k^G} b_{im} + a_{km}^{(2)}) \ \forall i \in \Omega^G \cup \Omega^{bus}, k \in \Omega^{bus} \tag{41}$$

where b_{im} in Eqns. (40) and (41) is the same as b_{im} in (28) and represents whether bus *k* is on the restoration path from initial bus *i* to generator *m*, while $a_{km}^{(2)}$ is the same as $a_{im}^{(2)}$ in (31) and indicates the state of bus *k* when generator *m* restarts. When $a_{km}^{(2)}=0$, bus *k* has not been re-energized. When bus *k* is located on the restoration path of generator *m* ($b_{im}=1$) and has not been re-energized ($a_{km}^{(2)}=0$), its start-up time is equal to the start-up time of generator *m*. The start-up times for the buses on the restoration path of generator *m* are all

the same as the start-up time for generator *m*; these are not the actual start-up times of the buses but rather are used to label the restoration path. The actual start-up times can be easily calculated from the restoration path matrix $B(i,m)$ after the GSUS is optimized.

3.7. Serial restoration constraint

As described subsection 3.5, we can obtain the start-up time for generator *m* (t_m^{start}) and the start-up time for the restoration path for restarting generator *m* (t_m^{path}). When the start-up time for the restoration path for restarting generator *m* (t_m^{path}) is not equal to the start-up time for another generator *g* (t_g^{start}), serial restoration is achieved. The above condition can be formulated as follows.

$$t_g^{start} - t_m^{path} - \varepsilon \le e_{gm}^{(1)} M_{19}, \ \forall m \in \Omega^G, g \in \Omega^G \tag{45}$$

$$t_m^{start} - t_g^{path} - \varepsilon \le e_{gm}^{(2)} M_{19}, \ \forall m \in \Omega^G, g \in \Omega^G \tag{46}$$

$$e_{gm}^{(1)} + e_{gm}^{(2)} = 1, \ \forall m \in \Omega^G, g \in \Omega^G \tag{47}$$

3.8. Constraints related to start-up time requirements

In the current research, the maximum and minimum restart time constraints (3) and (4) are not simultaneously expressed in a single model because these two constraints are mutually exclusive. In this paper, these two constraints are modeled as follows.

$$t_g^{start} - T_g^{\max} - \varepsilon \le e_g^{(1)} M_{20}, \ \forall g \in \Omega^G \tag{42}$$

$$T_g^{\min} - t_g^{\text{start}} - \varepsilon \le e_g^{(2)} M_{20}, \ \forall g \in \Omega^G \tag{43}$$

$$e_g^{(1)} + e_g^{(2)} = 1, \ \forall g \in \Omega^G \tag{44}$$

3.9. Transient frequency constraint

During the start-up of an NBS generator, the cranking power for the generator results in transient frequency deviations in the restored system. Therefore, it is necessary to check the transient frequency constraint for the restart of the NBS generators.

For the restored system, the transient frequency deviation can be formulated as follows [32]:

$$\frac{C_m}{\sum_{g \in \Omega_r^G} P_g / (df_g f_N)} \le \Delta f_{\lim}, \ \forall m \in \Omega^G \tag{48}$$

The maximum frequency deviation is set to 0.5 Hz in this study, and the value of df_g is discussed in [32].

Eqn. (48) cannot be directly used in this paper; instead, it is transformed into Eqn. (49) as follows.

$$C_m z_{mm}^{(2)} \le \Delta f_{\lim} \sum_{g \in \Omega_r^G} \frac{P_g (z_{gm}^{(3)} + z_{gm}^{(4)})}{df_g f_N}, \ \forall m \in \Omega^G \tag{49}$$

4. Solution Methodology

The proposed GSUS optimization model that considers flexible re-energizing times of transmission lines, as established in Section 3, is a MILP model that can be effectively solved using commercial solvers such as CPLEX. However, the number of constraints increases with the number of buses, which decreases the solution efficiency. Considering the characteristics of system restoration, some constraints can be neglected to improve the solution efficiency. Since the initial bus for restarting a new NBS generator must located at the edge of the restored network, buses that are not at the edge of the restored network cannot be chosen as this initial bus. Since the end bus for restarting a new NBS generator must be the bus connected to the generator, no bus that is not connected to an NBS generator can be chosen as such an end bus. Consequently, the constraints related to these buses can be neglected to reduce the number of constraints. Additionally, since only some of the constraints for system restoration are included in the proposed GSUS optimization model, the optimal result obtained from the proposed model may not satisfy other constraints for system restoration (such as the voltage security constraints and the power flow constraints); consequently, the solution should be corrected to ensure that it satisfies all of the constraints [32].

Accordingly, the solution procedure can be divided into four parts. The first step is data preparation, in which the system data and the restoration path and start-up time constraints are prepared. The second step involves searching for the critical buses and candidate restoration paths and generating restoration time and restoration path matrices to reduce the number of computations. The third step involves solving the GSUS optimization model. The last step involves repairing the GSUS scheme and generating the restoration plan.

The details of each step are given as follows, and a flow chart is shown in Fig. 3.

Step 1: Data preparation

Step 1.1: Input the data on the power network and the generators.

Step 1.2: Solve for the shortest path between each pair of buses using the *Floyd* algorithm.

Step 1.3: Establish the start-up time constraints for the generators.

Step 2: Search for critical buses and candidate restoration paths

Step 2.1: Remove restoration paths from bus k to NBS generator j whose restoration time T_{kj} is longer than the shortest restoration time T_{ij} between BS generator i and NBS generator j.

Step 2.2: Remove restoration paths starting from the NBS generators that connect to the power network via only one path.

Step 2.3: Search for buses that have no more than two adjacent buses. These buses are called middle buses in this paper.

Step 2.4: Remove all paths starting from middle buses.

Step 2.5: The buses on the remaining restoration paths are critical buses that are used as initial buses to restart the NBS generators. Moreover, the remaining paths are the candidate restoration paths.

Step 3: Calculate restoration time and restoration path matrices

Step 3.1: Generate the restoration time matrix $\boldsymbol{B}$ to calculate the fastest restoration time from critical bus i to NBS generator m among the candidate restoration paths identified in Step 2.5. If there is no candidate restoration path from critical bus i to NBS generator m, set the value of $\boldsymbol{B}(i,m)$ to 0. The fastest restoration time T_{im} in Eqn. (28) is equal to $\boldsymbol{B}(i,m)$.

Step 3.2: Generate the restoration path matrix $\boldsymbol{D}$ to count the critical buses that are located on the candidate restoration paths for each NBS generator. If critical bus i is located on a candidate restoration path for NBS generator m, set the value of $\boldsymbol{D}(i,m)$ to 1; otherwise, set this value to 0. Ω_k^G in Eqns. (35) and (36) can be obtained from the matrix $\boldsymbol{D}$.

Step 4: Establish and solve the proposed GSUS optimization model described in subsections 3.3 through 3.9

Step 5: Generate the restoration plan

Step 5.1: According to the GSUS generated in Step 4, dispatch the output power for the generators and the load pickup such that the operational constraints are satisfied, including the power flow constraints and the voltage security constraints. A method for generator dispatch and load restoration can be found in [31].

Step 5.2: Check whether all constraints are satisfied. If any constraint is not satisfied, repair the restoration plan. Some repair methods have been proposed in [29]. Following these repair methods, set new constraints for the transmission lines and NBS generators and return to Step 4. If all constraints are satisfied, output the restoration plan.

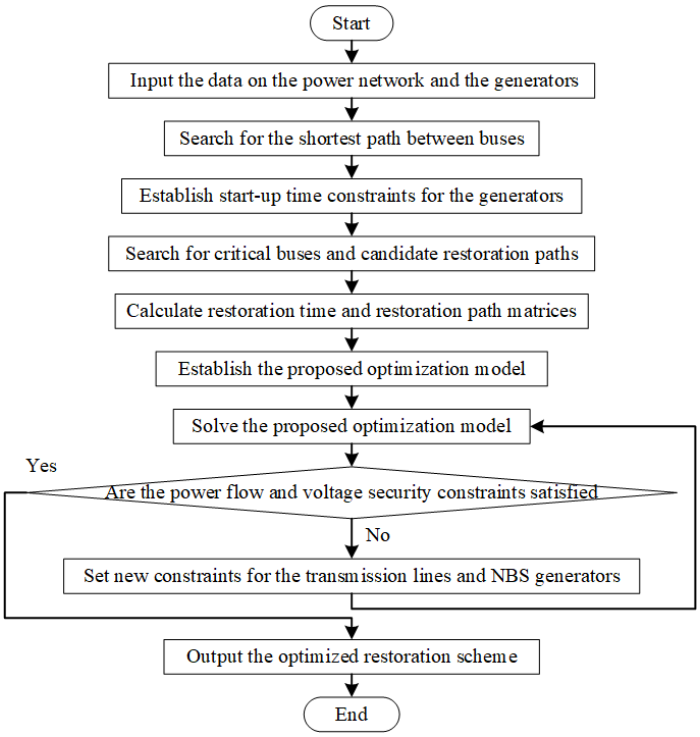

Fig. 3 Flowchart of the proposed solution method

5. Case Study

The proposed method was tested on the IEEE 39-bus system. The simulations were all performed in MATLAB using the CPLEX 12.2 solver on a PC with an Intel Core i7–6700HQ CPU (2.6 GHz) and 8 GB of memory. The solution results obtained using the proposed method are presented and analyzed. The advantages of the proposed method compared with the current method are verified.

5.1. Test system

The IEEE 39-bus system was used to verify the effectiveness of the proposed method. The topology of the test system is illustrated in Fig. 3. In the test system, the generator connected to bus 30 is a BS generator, and

the other generators are NBS generators. The start-up time for a generator is set to be the same as the start-up time for the bus connected to that generator, and the generator's number is set to the same value as the bus number. The parameters of the generators and transmission lines are shown in Table 1 and Appendix A, respectively. The values of M_5 and M_6 are both 360, the value of M_{15} is 140, and the values of the other M_x are all 150. The proposed model consists of 3436 constraints, 232 integer variables, and 1096 binary variables.

Table 1: Parameters of the generators

Gen.	T_g^{max} (min)	T_g^{min} (min)	Cranking time (min.)	Cranking power (MW)	Ramp rate (MW/min.)	P_{max} (MW)
30	-	-	0	0	2.5	450
31	60	100	35	26	2.9	572.9
32			38	30	3.1	650
33	50	70	30	25	2.6	508
34			40	28	3.0	632
35			36	31	3.3	650
36	30	60	29	25	2.7	560
37			29	28	2.7	540
38			45	31	3.6	830
39			55	40	4.4	1000

5.2. Solution results of the proposed method

In this simulation, the restoration time for each transmission line was set to 4 min as an example; however, other values can be set according to practical experience. The critical buses and candidate restoration paths were sought in the preparation stage following the proposed solution method, and matrices *B* and *D* are shown in Appendix B. In this case, the critical buses selected as the initial buses for NBS generator start-up were buses 2, 3, 4, 6, 10, 14, 16, 17, 19, 22, 23, 25, and 26. The optimized restoration paths obtained using the proposed method are shown in Fig. 3, where the red buses are middle buses, the blue buses are critical buses, and the NBS generators are listed in the start-up sequence. The detailed restoration scheme is shown in Table 2.

Table 2: Restoration scheme obtained with the proposed method

Generator	Start-up time (min.)	Restoration path
G37	12	30→2→25→37
G33	36	25→26→27→17→16→19→33
G39	44	2→1→39
G38	52	26→29→38
G34	60	19→20→34
G35	72	16→21→22→35
G36	80	22→23→36
G32	100	16→15→14→13→10→32
G31	112	10→11→6→31

The generator start-up sequence shown in Table 2 is a serial sequence that satisfies the serial restoration constraint. The restoration time for every generator considers the re-energizing times of the transmission lines. The initial buses for the NBS generators' restoration paths are all critical buses except for the BS generator. This means that the critical buses identified using the proposed method are effective for GSUS optimization. Out of all the NBS generators, G31, G33 and G36 have the maximum and minimum start-up time constraints. The start-up time for G33 is 36 min, which satisfies the maximum start-up time constraint. The start-up time for G31 is 112 min, and that for G36 is 80 min, satisfying the minimum start-up time constraint.

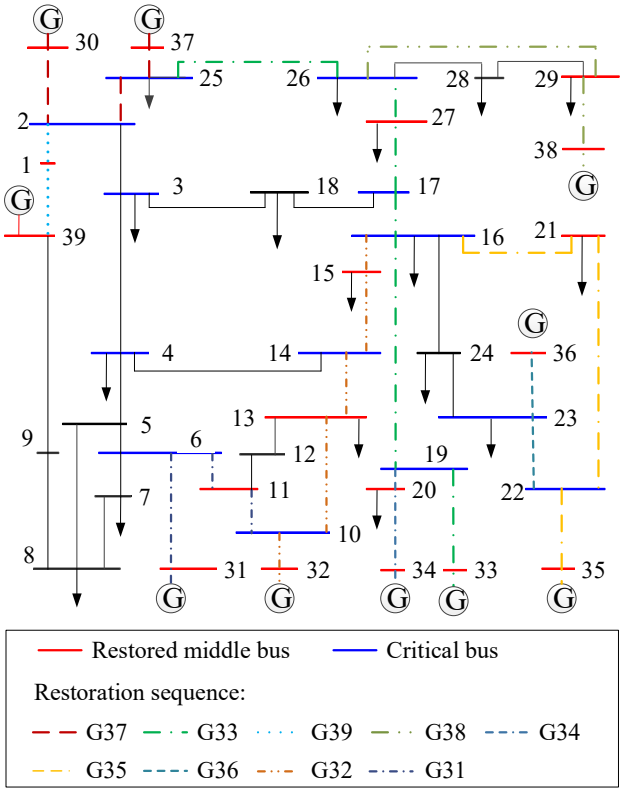

Fig. 4 Restoration path obtained using the proposed method

The available power in the restored system in the first 100 min is shown in Fig. 5. A drop in the available power curve indicates that an NBS generator has been restarted and is consuming cranking power. After the cranking period, the restored generator produces power and ramps up until it reaches its maximum power output, resulting in an increase in the available power indicated by the curve.

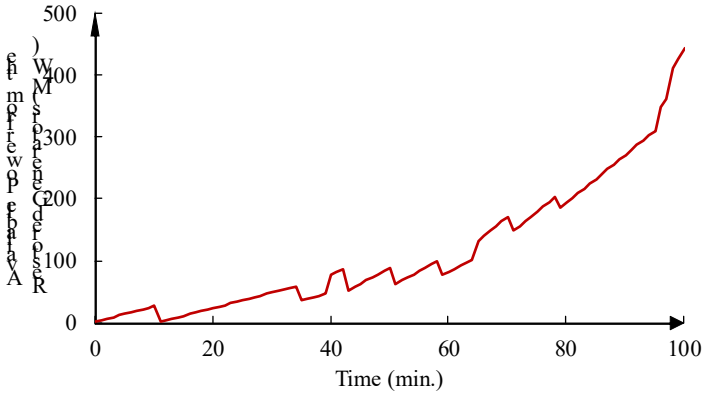

Fig. 5 Power available from the restored generators within the first 100 minutes

Since the re-energizing times for different transmission lines vary, the re-energizing time for each transmission line with a transformer was set to 6 min to simulate the flexible re-energizing time requirement.

The transmission lines with transformers are lines 30-2, 31-6, 32-10, 33-19, 34-20, 35-22, 36-23, 37-25, 38-29, 11-12, 12-13, and 19-20. The restoration scheme with flexible re-energizing times is shown in Table 3. The start-up times for the NBS generators are all later than those in the solution with equal re-energizing times as a result of the additional re-energizing time considered for the transformer branches. Moreover, the restoration sequence of the NBS generators is altered due to the additional re-energizing time for the transformer branches. These simulation results show that the proposed method can generate a start-up sequence for NBS generators considering flexible re-energizing times for the transmission lines.

Table 3: Restoration scheme with flexible re-energizing times

Generator	Start-up time (min.)	Restoration path
G37	16	30→2→25→37
G33	42	25→26→27→17→16→19→33
G39	50	2→1→39
G38	60	26→29→38
G35	74	16→21→22→35
G36	84	22→23→36
G34	96	19→20→34
G32	118	16→15→14→13→10→32
G31	132	10→11→6→31

5.3. *Comparison with the state-of-the-art methods*

In existing studies, several meta-heuristic algorithms have been employed to solve nonlinear models for GSUS optimization. Here, we take the artificial bee colony (ABC) algorithm [33] and the orthogonal genetic algorithm (OGA) [34] as examples to solve the original nonlinear model and compare the results with those of the proposed MILP model. The two-stage solution strategy in [15] was employed to implement both methods. In the first stage, the GSUS was separately optimized using either the ABC algorithm or the OGA, and then, the restoration paths were optimized in the second stage using the Floyd algorithm. Moreover, the MILP-based parallel GSUS optimized in [28] was improved by delaying the restart times of the parallel generators to generate a serial GSUS; the resulting solution is referred to as the improved parallel GSUS in the following paragraphs. The system parameters are the same as those in subsection 5.2, with flexible re-energizing times for the transmission lines.

The optimized restoration schemes corresponding to the ABC algorithm, the OGA and the improved parallel GSUS are shown in Table 4. The power generated with the different restoration schemes and the differences between the different restoration schemes are illustrated in Fig. 6. The dotted black, red, green and blue lines show the power generated with the proposed method, the improved parallel GSUS, the ABC algorithm and the OGA, respectively. The solid red line shows the difference between the solutions corresponding to the proposed method and the improved parallel GSUS. The solid green line shows the difference between the solutions obtained using the proposed method and the ABC algorithm. The solid blue line shows the difference between the solutions obtained using the proposed method and the OGA. The statistics of the different methods are summarized in Table 5.

Table 4: Optimized restoration schemes corresponding to the ABC, OGA and improved parallel GSUS solutions

ABC			OGA			Improved parallel GSUS		
Gen.	Start-up time (min.)	Restoration path	Gen.	Start-up time (min.)	Restoration path	Gen.	Start-up time (min.)	Restoration path
G37	16	30→2→25→37	G37	16	30→2→25→37	G37	16	30→2→25→37
G34	48	2→3→18→17→16→19→20→34	G33	42	2→3→18→17→16→19→33	G32	42	2→3→4→14→13→10→32
G39	56	2→1→39	G39	50	2→1→39	G39	50	2→1→39
G38	70	25→26→29→38	G38	64	25→26→29→38	G38	64	25→26→29→38
G33	76	19→33	G35	78	16→21→22→35	G33	86	3→18→17→16→19→33
G35	90	16→21→22→35	G36	88	22→23→36	G34	98	19→20→34
G36	100	22→23→36	G32	110	16→15→14→13→10→32	G35	112	16→21→22→35
G32	122	16→15→14→13→10→32	G31	124	10→11→6→31	G36	122	22→23→36
G31	136	10→11→6→31	G34	136	19→20→34	G31	136	10→11→6→31

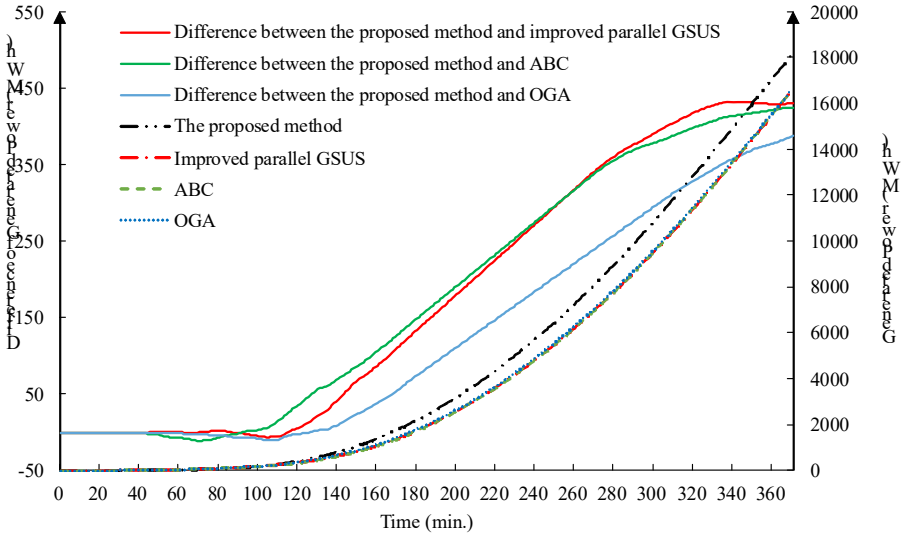

Fig. 6 Power generated with different restoration schemes

Table 5: Optimal results obtained with different methods

Algorithm	Objective value	Restoration scheme	Computation time
Proposed method	437911	30→37→33→39→38→35→36→34→32→31	236 seconds
Improved parallel GSUS	463718	30→37→32→39→38→33→34→35→36→31	207 seconds
ABC	463398	30→37→34→39→38→33→35→36→32→31	31072 seconds
OGA	461568	30→37→33→39→38→35→36→32→31→34	12912 seconds

Comparing Table 3 and Table 4, we can see that the restart times of the last generator are similar among the different methods. The last generator's restart time with the proposed method is only four minutes earlier than it is with the other methods. However, the start-up sequences and restoration sequences obtained using the different methods are different. Since generator G37 is close to the BS generator (G30), it is restarted first in all four schemes to increase the power quickly and decrease the wait times for the non-restored generators. The second generator to be restarted has a significant impact on the restoration efficiency of the different

schemes. Due to the minimum cold restart time and maximum hot restart time constraints, G33 is restarted within the maximum hot restart time in the schemes obtained using both the proposed method and the OGA. In the schemes corresponding to the ABC algorithm and the improved parallel GSUS, G32 and G34, without start-up time constraints, are restarted second, and all generators with start-up time constraints are restarted after the minimum cold restart time. Consequently, the power generated with the proposed method is less than that generated in the ABC from 42 min to 92 min, in the OGA solutions from 61 min to 125 min, and in the improved parallel GSUS from 89 min to 115 min, as shown in Fig. 6. However, after this short time period, the power generated with the proposed method is greater than that generated with the other methods since the generators that were started earlier enter their ramping periods.

Overall, the optimal results obtained with the proposed method are better than the results of the other methods. Moreover, the computation time of the proposed method is close to that of the improved parallel GSUS and much faster than those of the ABC algorithm and the OGA. The optimal results obtained with the ABC algorithm and the OGA are similar, but the computation time of the OGA is half that of the ABC algorithm since the OGA can generate initial and offspring populations that are scattered uniformly in the solution space and thus achieves a faster convergence speed. In summary, the proposed method achieves better optimization efficiency than the improved parallel GSUS, the ABC algorithm and the OGA.

6. Conclusion

A new MILP-based restoration planning method for serial GSUS optimization that considers flexible re-energizing times for transmission lines is proposed in this paper. The flexible re-energizing time and serial GSUS requirement are satisfied by means of a series of proposed constraints, including restoration time constraints for the transmission lines, start-up time constraints for the buses on the restoration paths, and a serial restoration constraint, that are formulated as mixed integer linear constraints by introducing auxiliary binary decision variables. The start-up power requirements and restart time constraints are transformed into a series of mixed integer linear constraints along with the transient frequency constraints. Simulation results obtained for the IEEE 39-bus system indicate that the proposed method can generate a serial restoration scheme for generator start-up while considering flexible re-energizing times for the transmission lines and achieves better restoration efficiency than existing methods.

In the method proposed in this study, the flexible re-energizing time and serial GSUS requirements are satisfied simultaneously, while the power flow and voltage security constraints are checked during load dispatch. The checking of the power flow and voltage security constraints and the dispatching of the loads should be incorporated into the MILP model to further improve the solution efficiency. Moreover, the uncertainties associated with renewable generators have not been integrated into the GSUS model. Future research should address these issues.

Appendix A

Data on transmission lines

Initial node of the line	End node of the line	Resistance (p.u.)	Reactance (p.u.)	Capacitance to ground (p.u.)	Transformer ratio
1	2	0.0035	0.0411	0.6987	0
1	39	0.001	0.025	0.75	0
2	3	0.0013	0.0151	0.2572	0
2	25	0.007	0.0086	0.146	0
2	30	0	0.0181	0	1.025
3	4	0.0013	0.0213	0.2214	0
3	18	0.0011	0.0133	0.2138	0
4	5	0.0008	0.0128	0.1342	0

4	14	0.0008	0.0129	0.1382	0
5	6	0.0002	0.0026	0.0434	0
5	8	0.0008	0.0112	0.1476	0
6	7	0.0006	0.0092	0.113	0
6	11	0.0007	0.0082	0.1389	0
6	31	0	0.025	0	1.07
7	8	0.0004	0.0046	0.078	0
8	9	0.0023	0.0363	0.3804	0
9	39	0.001	0.025	1.2	0
10	11	0.0004	0.0043	0.0729	0
10	13	0.0004	0.0043	0.0729	0
10	32	0	0.02	0	1.07
12	11	0.0016	0.0435	0	1.006
12	13	0.0016	0.0435	0	1.006
13	14	0.0009	0.0101	0.1723	0
14	15	0.0018	0.0217	0.366	0
15	16	0.0009	0.0094	0.171	0
16	17	0.0007	0.0089	0.1342	0
16	19	0.0016	0.0195	0.304	0
16	21	0.0008	0.0135	0.2548	0
16	24	0.0003	0.0059	0.068	0
17	18	0.0007	0.0082	0.1319	0
17	27	0.0013	0.0173	0.3216	0
19	20	0.0007	0.0138	0	1.06
19	33	0.0007	0.0142	0	1.07
20	34	0.0009	0.018	0	1.009
21	22	0.0008	0.014	0.2565	0
22	23	0.0006	0.0096	0.1846	0
22	35	0	0.0143	0	1.025
23	24	0.0022	0.035	0.361	0
23	36	0.0005	0.0272	0	1
25	26	0.0032	0.0323	0.531	0
25	37	0.0006	0.0232	0	1.025
26	27	0.0014	0.0147	0.2396	0
26	28	0.0043	0.0474	0.7802	0
26	29	0.0057	0.0625	1.029	0
28	29	0.0014	0.0151	0.249	0
29	38	0.0008	0.0156	0	1.025

Appendix B

Matrix *B*: Times required for the candidate restoration paths for each NBS

End / Start	31	32	33	34	35	36	37	38	39
30	24	28	32	36	36	36	12	20	12
2	20	24	28	32	32	32	8	16	8
3	16	20	24	28	28	28			
4	12	16	20	24	24	24			
6		12							
10	12								
14	16	12	16	20	20	20			
16		20	8	12	12	12			
17			24	12	16	16			

19			4	8					
22						8			
23					8				
25			24	28	28	28	4	12	
26			20	24	24	24		8	

Matrix *D*: Nodes on the candidate recovery paths for each NBS

End Path node	31	32	33	34	35	36	37	38	39
2	1	1	1	1	1	1	1	1	1
3	1	1	1	1	1	1	0	0	0
4	1	1	0	0	0	0	0	0	0
6	1	0	0	0	0	0	0	0	0
10	0	1	0	0	0	0	0	0	0
14	0	1	1	1	1	1	0	0	0
16	0	0	1	1	1	1	0	0	0
17	0	0	1	1	1	1	0	0	0
19	0	0	1	1	0	0	0	0	0
22	0	0	0	0	1	0	0	0	0
23	0	0	0	0	0	1	0	0	0
25	0	0	1	1	1	1	1	1	0
26	0	0	0	0	0	0	0	1	0

Acknowledgments

This work is supported by the National Natural Science Foundation of China (51977111,61673213) and The Fundamental Research Funds for the Central Universities (30918011330). The authors would also like to thank the editor and anonymous reviewers for their comments to improve this paper.

References

[1] Wang Y, Chen C, Wang J, et al. Research on resilience of power systems under natural disasters-A review[J]. IEEE Transactions on Power Systems, 2015, 31(2): 1604-1613.

[2] Goswami D. A 10-step plan to end India's blackout[J]. Renewable Energy Focus, 2012, 13(5): 26-28.

[3] Black System South Australia 28 September 2016-Final Report[R]. March, 2017, [Online] Available: https://www.aemo.com.au/-/media/Files/Electricity/NEM/Market_Notices_and_Events/Power_System_Incident_Reports/2017/Integrated-Final-Report-SA-Black-System-28-September-2016.pdf.

[4] Erik Linask. Line failure causes massive power outage across Brazil[R]. Power Protection, March, 23, 2018, [Online] Available: https://www.powerprotectionresource.com/articles/437577-line-failure-causes-massive-power-outage-across-brazil.htm

[5] Oxford Analytica. Blackout hits Macri's hope of re-election in Argentina[R]. Emerald Expert Briefings, [Online] Available: https://www.emerald.com/insight/content/doi/10.1108/OXAN-ES244559/full/html.

[6] Bie Z, Lin Y, Li G, et al. Battling the extreme: A study on the power system resilience[J]. Proceedings of the IEEE, 2017, 105(7): 1253–1266.

[7] Liu W, Lin Z, Wen F, et al. A wide area monitoring system based load restoration method[J]. IEEE Transactions on Power Systems, 2013, 28(2): 2025-2034.

[8] Adibi M M . Power system restoration—A task force report[J]. IEEE Transactions on Power Systems, 1987, PWRS-2(2): 271–277.

[9] Sarmadi S A N, Dobakhshari A S, Azizi S, et al. A sectionalizing method in power system restoration based on WAMS[J]. IEEE Transactions on Smart Grid, 2011, 2(1): 190-197.

[10] Quirós-Tortós J, Wall P, Ding L, et al. Determination of sectionalising strategies for parallel power system restoration: A spectral clustering-based methodology[J]. Electric Power Systems Research, 2014, 116: 381-390.
[11] Wang C, Vittal V, Sun K. OBDD-based sectionalizing strategies for parallel power system restoration[J]. IEEE Transactions on Power Systems, 2011, 26(3): 1426-1433.
[12] Lin Z, Wen F, Chung C Y, et al. Division algorithm and interconnection strategy of restoration subsystems based on complex network theory[J]. IET Generation, Transmission & Distribution, 2011, 5(6): 674-683.
[13] Hazarika D, Sinha A K. Power system restoration: planning and simulation[J]. International journal of electrical power & energy systems, 2003, 25(3): 209-218.
[14] Zhao J, Wang H, Liu Y, et al. Coordinated restoration of transmission and distribution system using decentralized scheme[J]. IEEE Transactions on Power Systems, 2019, 34(5): 3428-3442.
[15] Zhang C, Lin Z, Wen F, et al. Two-stage power network reconfiguration strategy considering node importance and restored generation capacity[J]. IET Generation, Transmission & Distribution, 2014, 8(1): 91-103.
[16] Golshani A, Sun W, Zhou Q, et al. Incorporating wind energy in power system restoration planning[J]. IEEE Transactions on Smart Grid, 2017, 10(1): 16-28.
[17] Liu W, Sun L, Lin Z, et al. Multi-objective restoration optimisation of power systems with battery energy storage systems[J]. IET Generation, Transmission & Distribution, 2016, 10(7): 1749-1757.
[18] Gholami A, Aminifar F. A hierarchical response-based approach to the load restoration problem[J]. IEEE Transactions on Smart Grid, 2015, 8(4): 1700-1709.
[19] Xie Y, Liu C, Wu Q, et al. Optimized dispatch of wind farms with power control capability for power system restoration[J]. Journal of Modern Power Systems and Clean Energy, 2017, 5(6): 908-916.
[20] Zhao J, Wang H, Liu Y, et al. Utility-oriented online load restoration considering wind power penetration[J]. IEEE Transactions on Sustainable Energy, 2018, 10(2): 706-717.
[21]Sakaguchi T, Matsumoto K, Development of a Knowledge Based System for Power System Restoration[J]. IEEE Transactions on Power Apparatus and System, 1983, PAS-102(2): 320-329.
[22]Bang Z, Hope G, Malik O. A Knowledge-based Approach to Optimize Switching in Substations[J]. IEEE Transactions on Power Delivery, 1990, 5(1).
[23] Kirschen D S, Volkmann T L. Guiding a power system restoration with an expert system[J]. IEEE Transactions on Power System, 1991, 6(2): 558-566.
[24] Hou J, Xu Z, Dong Z Y, et al. Permutation-based power system restoration in smart grid considering load prioritization[J]. Electric Power Components and System, 2014, 42(3-4): 361-371.
[25] El-Zonkoly A M. Renewable energy sources for complete optimal power system black-start restoration[J]. IET Generation, Transmission & Distribution, 2014, 9(6): 531-539.
[26] Liu W, Sun L, Lin Z, et al. Multi-objective restoration optimisation of power systems with battery energy storage systems[J]. IET Generation, Transmission & Distribution, 2016, 10(7): 1749-1757.
[27] Zhang C, Lin Z, Wen F, et al. Two-stage power network reconfiguration strategy considering node importance and restored generation capacity[J]. IET Generation, Transmission & Distribution, 2014, 8(1): 91-103.
[28] Sun W, Liu C C, Zhang L. Optimal generator start-up strategy for bulk power system restoration[J]. IEEE Transactions on Power System, 2010, 26(3): 1357-1366.
[29] Qiu F, Li P. An integrated approach for power system restoration planning[J]. Proceedings of the IEEE, 2017, 105(7): 1234-1252.
[30] Jiang Y, Chen S, Liu C C, et al. Blackstart capability planning for power system restoration[J]. International Journal of Electrical Power & Energy System, 2017, 86: 127-137.
[31] Sun L, Lin Z, Xu Y, et al. Optimal skeleton-network restoration considering generator start-up sequence and load pickup[J]. IEEE Transactions on Smart Grid, 2019, 10(3): 3174-3185.
[32] Adibi M M, Borkoski J N, Kafka R J, et al. Frequency response of prime movers during restoration[J]. IEEE Transactions on Power system, 1999, 14(2): 751-756.
[33] Xu K, Xie B, Wang C, et al. An ABC algorithm for optimization of restoration path in a power grid with HVDC connection[C]// IEEE International Conference on Smart Grid Communications, 2016: 576-581.
[34] Xie Y, Song K, Wu Q, et al. Orthogonal genetic algorithm based power system restoration path optimization[J]. International Transactions on Electrical Energy Systems, 2018: e2630.